JOURNAL OF CATALYSIS 67, 77–89 (1981)

Electrocatalytic Hydrogenation of Ethylene over Palladium at Positive Potentials

GEORGE P. SAKELLAROPOULOS[1] AND STANLEY H. LANGER

Department of Chemical Engineering, University of Wisconsin, Madison, Wisconsin 53706

Received February 26, 1979; revised July 15, 1980

The palladium-black-catalyzed electrogenerative hydrogenation of ethylene was investigated over partially wettable, porous, commercial electrodes between +0.6 and 0 V. In perchloric acid electrolyte, hydrogen ion transport in the catalyst pores was rapid, but ethylene pore diffusion became rate limiting below 0.3 atm partial pressure. A simple pore model treatment allows the incorporation of an electrochemical Thiele modulus. With this treatment, the evaluation of intrinsic electrode kinetic parameters from apparent ones is demonstrated. A mechanistic model is proposed involving the surface insertion of ethylene to adsorbed hydrogen atoms followed by slow hydrogen addition to the resulting surface ethyl radicals. This model is used to explain differences in reaction rate, overpotential, and selectivity for double bond reduction on palladium and platinum.

INTRODUCTION

The role of catalysts in electrochemical, energy-generating, organic reactions other than complete oxidation is still in the process of elucidation. Platinum is the most well-characterized electrocatalyst; information on other catalysts is limited. We have found the electrogenerative hydrogenation of ethylene, involving a hydrogen anode with an ethylene cathode and acid electrolyte, to be particularly convenient for electrocatalysis studies. Results from the electrocatalyzed electrogenerative hydrogenation of simple and substituted alkenes showed that both reaction rates (*1*) and selectivities (*2*) varied with the noble metal catalyst employed, particularly for palladium and platinum. Similar electrocatalytic behavior was observed in fuel cell hydrocarbon oxidations (*3*). To understand such differences, more detailed knowledge of surface reactions on noble metal electrocatalysts is required. To clarify some of these surface processes, we previously described studies of electrogenerative hydrogenation on platinum-black (*4*, *5*). Here we report results for palladium-black, porous electrocatalysts.

One advantage of studying the electrogenerative hydrogenation of ethylene is the possibility of comparing results with the extensive information obtained from conventional catalytic hydrogenation. Since the intrinsic reduction rate is faster on palladium-black than on platinum (*1*), development of pore diffusion limitations was anticipated at lower current densities on the former. The relatively simple ethylene reduction, compared to fuel cell oxidation reactions, allows less ambiguous interpretation of rate parameters with porous electrodes; it also provides a possibility for testing a previously proposed simple pore model (*6*). Kinetic investigations on porous electrocatalysts are important for electrogenerative and fuel cell design to reconcile differences in activity or mechanism between porous and smooth, planar electrodes (*4*). The former are more efficient for energy generation.

During electrogenerative hydrogenation, the catalytic cathode operates at positive potentials with respect to the hydrogen anode (*2*, *4*). Olefin substrate and hydrogen are separated by an electrolyte barrier with

[1] Present address: Department of Chemical and Environmental Engineering, Rensselaer Polytechnic Institute, Troy, N.Y. 12180.

0021-9517/81/010077-13$02.00/0

the generated current from alkane formation carried through an external circuit. In contrast, the potentiometric method requires an external power source and dissolution of substrate; electrochemical as well as chemical hydrogenation can take place simultaneously (*7, 8*).

The use of perchloric acid as electrolyte in this work tends to minimize undesired side reactions or catalyst inhibition from strong anion adsorption, such as may occur with chloride ions (*9*). Such adsorption is probable (*9*) in the earlier investigation of electrochemical ethylene reduction at palladium electrodes in HCl solution by Burke *et al.* (10). To our knowledge no other kinetic or mass transport analysis has been presented on the electrocatalytic hydrogenation of alkenes over porous or smooth palladium electrodes at positive potentials.

METHODS

A matrix cell was used with the cathode and anode separated by an electrolyte barrier supported on five disks on filter paper, Whatman No. 42 (*1, 5*). The cathode was a commercial polytetrafluoroethylene-bonded partially wettable porous electrode activated with 9 mg Pd/cm^2 (American Cyanamid, Type AA-2) (*11*). The anode was of similar type, but activated with 9 mg Pt/cm^2.

The cell was connected to an all-glass-and-Teflon system (*2, 4*) which permitted purging and pretreatment of both electrodes with nitrogen or hydrogen without atmospheric contact. Gases and electrolytes used here and methods for preparing gas mixtures have been described previously (*4*).

The electrolyte ionic strength was maintained constant at that of a 2 N solution by using appropriate $HClO_4$–$LiClO_4$ mixtures. High ionic strength at low acid concentrations tends to maintain the electrical character of the diffuse double layer and minimizes potential drop across it (*4*).

To remove oxygen traces from ethylene and nitrogen, the gases were passed through an alkaline pyrogallol solution followed by calcium sulfate and molecular sieve 13X columns. They were then saturated with water before entering the cell to avoid matrix drying or electrolyte concentration change. Typical gas flow rates were about 8 ml/min for ethylene–nitrogen mixtures. This excess gas flow ensured that both kinetic and limiting currents were independent of gas rate. The effluent gas stream was analyzed by gas chromatography (Porapak QS, 6-ft × $\frac{1}{8}$-in. column) (4).

The electrical equipment and the experimental procedure have been described before (*4*). After the cell was assembled, both anode and cathode electrocatalysts were pretreated first with nitrogen and then with hydrogen, while the electric circuit was shorted. This procedure eliminated oxygen traces and impurities from the electrolyte and the catalyst surface before potential–current density data were obtained. After the hydrogen pretreatment the cell internal resistance was measured (*4*). The cell resistance was usually constant throughout each experiment.

The reported cell voltage and current represent steady-state values, normally reached within 3 min of operation at a given current. The cell voltage was corrected for ohmic losses in the electrolyte and for concentration polarization associated with the limiting current (*4*).

$$E_c = E_m + iA_g R_i - \frac{RT}{nF} \ln \left(\frac{i_L - i}{i_L} \right). \quad (1)$$

Here E_c is the corrected cathode voltage in volts, E_m the measured cell voltage, R_i the measured internal resistance of the cell, A_g the exposed geometric electrode area (5.07 cm^2), i the current density based on the geometric area, i_L the limiting current density, and n the number of electrons involved in the electrochemical step, e.g., $n = 2$ for ethylene reduction. The cathode potential E was then obtained by correcting for the hydrogen anode polarization. The latter was about 8 mV per decade (*4*). Cathode potentials are reported here with

reference to the normal hydrogen electrode (NHE) by correcting for the potential change of the cell hydrogen electrode with H^+ concentration, using the Nernst equation.

RESULTS

The steady-state cell voltage under load deviates considerably from its rest value, Fig. 1. Similar behavior is observed on platinum-black cathodes (*4*) but at voltages 40–50 mV lower than on palladium. Between 0.6 and 0.26 V the cathode potential is neither a linear nor a logarithmic function of the current density. Below 0.26 V, a Tafel logarithmic dependence is observed at constant electrolyte and ethylene concentration so that

$$i_g = nFk^0 \Pi C_j^j \exp\left(-\frac{\alpha FE}{RT}\right), \qquad (2)$$

where i_g is the observed current density, k^0 the heterogeneous rate constant at zero electrode potential vs NHE, j the reaction order in species J, and α the transfer coefficient. From a semilogarithmic plot of potential vs current (Tafel plot) the Tafel slope ($RT/\alpha F$) and the transfer coefficient can be determined experimentally. These parameters provide information on the rate-determining step in an electrochemical mechanism sequence (*12*). The observed Tafel behavior and the slope of 0.033 V here suggest an irreversible, two-electron electrochemical reaction with the second electron transfer slow. This result is in agreement with other kinetic information discussed later.

The position of the Tafel curves, Fig. 2, and their slopes are reproducible within 5–10% in independent experiments. Reproducibility of results even after prolonged use of the electrocatalyst (~80 h) indicates that little catalyst deactivation occurred during this work. Deactivation would be indicated by decreased current density at a given potential.

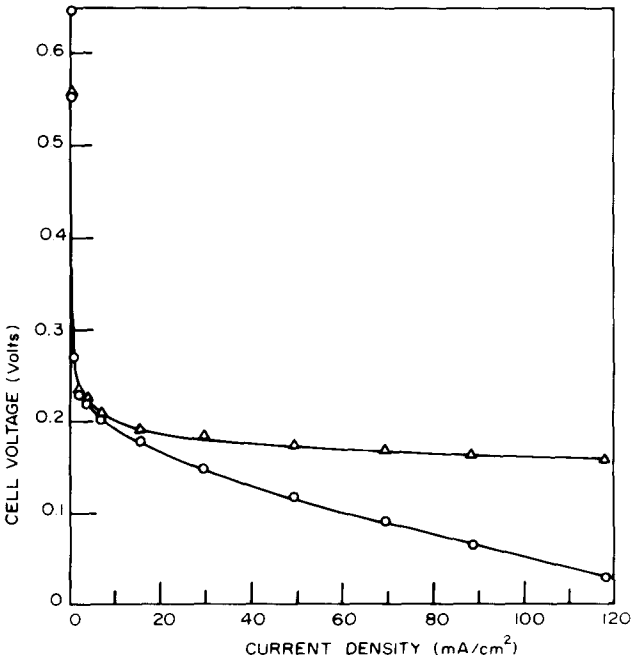

FIG. 1. Potential–current density curve for ethylene electrogenerative hydrogenation on palladium-black. Electrolyte, 2 *N* $HClO_4$ supported on matrix; cell internal resistance, 0.238 Ω; temperature, 24°C. (○) Measured voltage; (△) ir-corrected voltage.

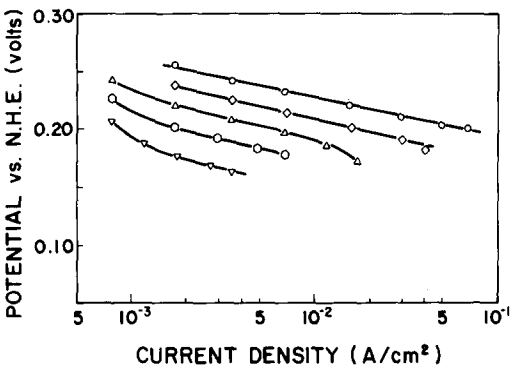

FIG. 2. Effect of electrolyte concentration on palladium cathode potential. Electrolyte, aqueous $HClO_4$–$LiClO_4$; temperature, 24°C. (○) 2 *N* $HClO_4$; (◇) 1 *N*; (△) 0.5 *N*; (○) 0.2 *N*; (▽) 0.1 *N*.

The reaction rate decreases with decreasing hydrogen ion concentration, Fig. 2. At the approach of a limiting current, slow ion diffusion results in concentration overpotential. After correction of the cathode potential for Nernst diffusion (limiting current term, Eq. (1)) the intrinsic Tafel slope of 0.033 V is observed.

With decreasing ethylene partial pressure in inert nitrogen, at a high H^+ concentration (2 *N* $HClO_4$), there is a decrease in reaction rates and a gradual change of the Tafel slopes, Fig. 3. This is especially evident at $P_{C_2H_4} < 0.3$ atm. At low ethylene partial pressures and cathode potentials below 0.07 V the hydrogen evolution reaction (HER) driven by concentration effects becomes significant. Similar results are observed on platinum in the same potential region (*4*). The HER occurs at about the same potential, regardless of whether pure nitrogen or a dilute ethylene–nitrogen mixture is used on the cathode (*1*, *4*). Since its rate is 2 to 3 orders of magnitude lower than the ethylene hydrogenation rate in the Tafel region, the HER can be neglected in that region.

Assuming a simple exponential rate equation (cf. Eq. (2)), reaction orders can be estimated from known reaction rates or current densities:

$$\left(\frac{\partial \log i}{\partial \log C_J}\right)_{T,E,C_{k\neq J}} = j. \qquad (3)$$

The order j in species J is obtained at constant temperature, potential, electrolyte ionic strength, and concentrations of other reactants. Analysis of Fig. 4 shows that the assumption of simple order reaction is reasonable for the hydrogen ion reactant in the studied concentration range. From this

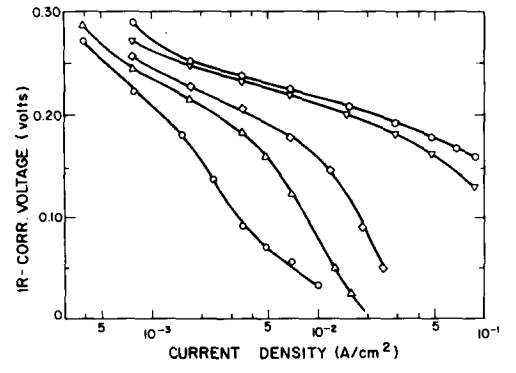

FIG. 3. Effect of ethylene partial pressure on cathode potential. Electrolyte, 2 *N* $HClO_4$; temperature, 24°C. (○) $P_{C_2H_4}$ = 1 atm; (▽) 0.29; (◇) 0.013; (△) 0.056; (○) 0.027.

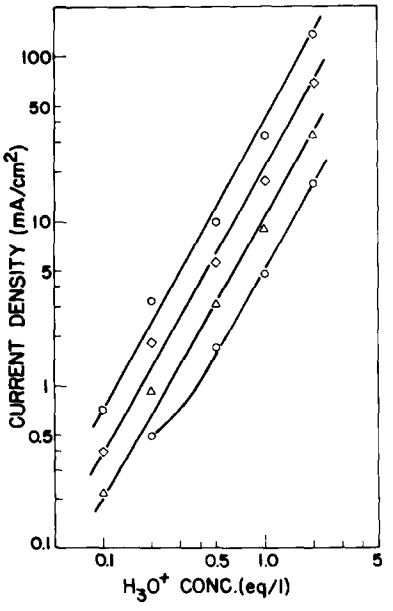

FIG. 4. Reaction rate vs electrolyte concentration at constant potentials. Cathode: Palladium 9 mg/cm²; $P_{C_2H_4}$ = 1 atm; temperature, 25°C. (○) *E* = 0.19 V; (◇) 0.20; (△) 0.21; (○) 0.22 V vs NHE.

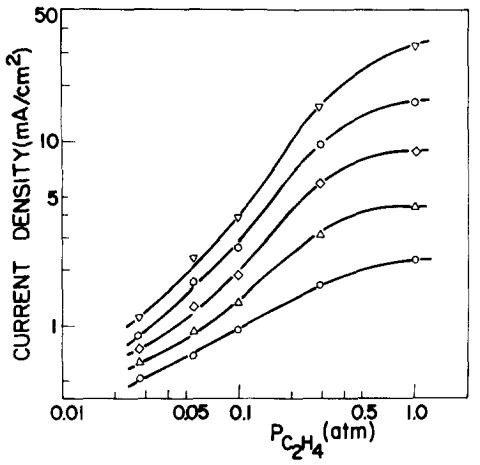

FIG. 5. Reaction rate vs ethylene partial pressure at constant potential. Electrolyte, 2 N $HClO_4$; temperature, 24°C. (▽) E = 0.21 V; (○) 0.22; (◇) 0.23; (△) 0.24; (○) 0.25 V vs DHE.

figure, the reaction order with respect to hydrogen ions is obtained as the slope.

Results are more complex with ethylene. For partial pressures above 0.3 atm and potentials about 0.25 V the order is effectively zero. Below this pressure and at the same potential (0.25 V), an order of 0.4 is obtained from the slope of the corresponding line of Fig. 5. At lower potentials, curved lines are obtained. Equation (3) no longer applies nor can a Hougen–Watson adsorption model explain these results. One viable explanation is in terms of slow pore diffusion superimposed on the intrinsic kinetics (*6*), as discussed below. Table 1 summarizes intrinsic kinetic parameters for ethylene hydrogenation on palladium-black electrocatalyst.

DISCUSSION

Reaction Kinetics and Pore Diffusion

When using porous electrocatalysts for kinetic investigations some attention should be given to recognizing possible slow pore diffusion of reactants. Slow mass transport into the pores can interact with the intrinsic reaction kinetics to alter reaction orders, Tafel slopes, and energies of activation (*6*). With the relatively simple ethylene hydrogenation reaction, slow pore diffusion can be identified when it is important.

The reaction order in hydrogen ions, Table 1, differs from the nearest integer value by less than 10% and is constant for all potentials. An assumption of negligible ohmic losses in the pores seems justified since no change of the Tafel slopes is observed at low electrolyte concentrations (0.1 to 0.5 N $HClO_4$) for which resistivity is 4 to 6 times higher than in 2 N $HClO_4$. Therefore, hydrogen ion diffusion into the pores is fast and essentially constant H^+

TABLE 1

Kinetic Parameters for Electrogenerative Hydrogenation of Ethylene on Palladium-Black

Reaction rate: $i = nFk^0C_{H^+}^b P_{C_2H_4}^a \exp\left(-\frac{\alpha EF}{RT}\right)$

Parameter	Experimental intrinsic	Experimental apparent	Theoretical apparent
Reaction order in H^+, b	1.8	—	—
Reaction order in C_2H_4, a	0	0.4	0.5
Transfer coefficient, α	1.78	0.82	0.89
Tafel slope ($2.3RT/\alpha F$) (V)	0.033	0.072	0.066
Rate constant at zero potential, k_0 (cm^4/mole · s)	1×10^5	—	—
Standard exchange current density, i_0 (A/cm^2)[a]	3×10^{-6}	—	—

[a] $i_0 = nFk_0 \exp(-\alpha E^0 F/RT)$.

concentration is maintained. Fast hydrogen ion diffusion results in complete utilization of the electrolyte-filled pores by the reactants (H^+ and dissolved C_2H_4) at high ethylene partial pressures and examined H^+ concentrations, a behavior also observed with platinum-black (*4*).

To explain results at low ethylene partial pressures, slow pore diffusion of ethylene should be considered. For this, adoption of a porous electrocatalyst model is useful. In a recent discussion of electrode kinetics we employed the simple pore model for our analysis (*6*) because of its similarity to slab geometry models for conventional heterogeneous catalysts (*13, 14*). Similar results would be obtained with a thin film model (*15*) if diffusion of the gaseous reactant in the radial direction, across the thin film, is assumed fast. The assumption here of slow diffusion only in the axial direction seems plausible for low ethylene partial pressures, where inert nitrogen and product ethane can "blanket" the interior of the pores. With the high electrolyte conductivity, low current, and the open electrode porosity, ohmic lossses in the pores can be neglected (*6*).

The local current density (rate) in the pores for a jth-order irreversible electrocatalytic reaction would be

$$\bar{i}_x = nFk_j{}^0C_J{}^j \exp(-\alpha\, EF/RT), \quad (4)$$

where C_J is the local concentration of species J and $k_J{}^0$ contains any constant concentration terms; e.g., here $k_J{}^0 = k^0C_{H^+}{}^2$.

A mass balance on reactant in a pore gives in dimensionless form (*6*)

$$\frac{d^2\Psi_J}{dX^{*2}} - h^2\Psi_J{}^j = 0, \quad (5)$$

$$\Psi_J = 1 \text{ at } X^* = 0; \qquad \frac{d\Psi_J}{dX^*} = 0 \text{ at } X^* = 1, \quad (6)$$

where $\Psi_J = C_J/C_{J\infty}$ is the dimensionless concentration, and $X^* = X/L$ the dimensionless length. The "electrochemical Thiele modulus," h, becomes a function of the reactant bulk concentration, $C_{J\infty}$, and the electrode potential

$$h = L\left[\frac{2k_J{}^0C_{J\infty}{}^{j-1}}{\mathscr{D}_jR_p}\exp\left(-\frac{\alpha EF}{RT}\right)\right]^{1/2}. \quad (7)$$

Here $C_{J\infty}$ is the ethylene concentration in the electrolyte, in equilibrium with the gas-phase concentration. Assuming Henry's law, $C_{J\infty} = K_HP_{J\infty}$. The constant K_H is 6.1×10^{-6} mole/ml (*16*).

For a zero-order reaction, the pore utilization is complete if $h \leq 2^{1/2}$ (*17*) and intrinsic kinetics are observed. If $h > 2^{1/2}$, solution of Eq. (5) gives the concentration profile in the pores (*6*). The apparent rate, i_g, is then

$$i_g = nFk_j{}^0C_{J\infty}{}^j\left(\frac{2^{1/2}}{h}\right)\exp(-\alpha EF/RT). \quad (8)$$

The term $\epsilon = 2^{1/2}/h$ is an "electrochemical effectiveness factor," dependent not only on concentration but also on potential (*6*). From Eqs. (7) and (8), the observed apparent kinetic parameters for a zero-order reaction become (*6, 17*)

$$j' = 0.5, \alpha' = \alpha/2.$$

The experimental orders in ethylene at high potentials (~0.25 V) are in agreement with this theoretical model. The order is zero at $P_{C_2H_4} > 0.3$ atm and becomes 0.4 at low pressures. Similarly, at high ethylene partial pressures and for all electrolyte concentrations, the Tafel slopes are ~0.033 V. The observed Tafel slopes at $P_{C_2H_4} < 0.3$ atm gradually increase to 0.072 V, reflecting transition from kinetic to pore diffusion control at low pressures. Because of this transition and the changed Tafel slopes, no simple correlation should be anticipated between reaction rate and low ethylene partial pressure (cf. Fig. 5, at potentials below 0.25 V).

The model above can be tested by determining electrochemical effectiveness factors at varying ethylene partial pressures and potentials. The electrochemical effectiveness factor can be expressed as the

ratio of the pore diffusion controlled rate (current density) at pressure P, i_P, to the intrinsic one at one atm, i_1:

$$\epsilon = \left(\frac{i_p}{i_1}\right)_{T,E,C_{H^+}} = \frac{2^{1/2}}{h}. \qquad (9)$$

Recently we have used results from the ethylene hydrogenation on palladium to demonstrate the validity of Eq. (8) for a zero-order reaction (*6*, *17*). The ratio i_P/i_1 was plotted against the parameters $P_{C_2H_4}$ and E as predicted by Eqs. (7) and (9). The experimental points were in very good agreement with the theoretical model (*6*), showing a significant decrease in pore utilization with decreasing ethylene partial pressure and potential. The fact that the electrochemical reactor provides the reaction rate directly as current density, makes electrochemical techniques useful tools for investigations of porous, conductive catalysts.

Open-Circuit Voltage

The open-circuit voltage (OCV) of the cell varies with electrolyte concentration, Table 2, showing a Nernstian behavior:

$$\frac{\partial E_{OCV}}{\partial \ln C_{H^+(T,P_{C_2H_4})}} = \frac{RT}{F}. \qquad (10)$$

Similar change was reported earlier for platinum (*4*). At ethylene partial pressures below 0.1 atm, the OCV varies with $P_{C_2H_4}$ following an equation similar to (10), in contrast to platinum, on which no OCV change is observed (*4*). At high partial pressures, however, the OCV becomes significantly higher than anticipated from the Nernst equation. The observed differences in OCV between palladium and platinum are in accord with the weaker ethylene adsorption strength on palladium relative to platinum (*8*). Weakly adsorbed ethylene probably cannot displace hydrogen dissolved in or adsorbed on palladium at low $P_{C_2H_4}$, yielding lower rest potentials. Increasing ethylene partial pressure may expedite surface hydrogen displacement resulting in higher OCV. Weak ethylene adsorption on palladium is further supported by an observed slower rate of approach of the steady-state OCV on palladium compared to platinum.

TABLE 2

Open-Circuit Voltage Change with H^+ and C_2H_4 Concentration

H^+ concn[a] (geq/liter)	OCV[b] (V)	$P_{C_2H_4}$ (atm)[c]	OCV[b] (V)
2.0	0.662	0.290	0.590
1.0	0.632	0.103	0.492
0.5	0.610	0.066	0.468
0.2	0.586	0.028	0.448

[a] At constant $P_{C_2H_4}$ = 1 atm.
[b] Measured voltage against a hydrogen anode electrode in the same electrolyte at zero current.
[c] At constant C_{H^+} = 2 geq/liter.

Limiting Currents

The reaction rate for ethylene hydrogenation controlled by potential reaches a limiting value at low reactant or electrolyte concentrations, as limiting currents associated with slow ionic transport are observed in the matrix-supported electrolyte even with 1 N $HClO_4$. In contrast to this, ionic transport in unsupported, free electrolytes is enhanced by free convection and limitations develop only below 0.5 N H^+ concentrations (*17*). Correction of the observed limiting currents here for the small contribution of migration (5–10%), as outlined previously (*17*), gives a linear dependence of the limiting current density on H^+ concentration ($i_L \propto C_{H^+}$). This suggests that diffusion through a stagnant layer is the main transport mechanism for H^+ in the supported electrolyte, at high currents and low acid concentrations (*17*).

Limiting currents at low ethylene partial pressures obey a relationship of the form

$$i_L \propto P_{C_2H_4}^{1.5}. \qquad (11)$$

Similar behavior was observed on platinum (*4*). The form of Eq. (11) results from the

variation of the available pore area with ethylene concentration as discussed elsewhere (*17*).

Kinetic Model

The intrinsic reaction rate in terms of current density is given by Eq. (12), if the experimental kinetic parameters of Table 1 are approximated by closest integers

$$i = nFk^0 P^0_{C_2H_4} C_{H^+}{}^{+2} \exp(-2EF/RT). \quad (12)$$

Reaction orders and transfer coefficient suggest that hydrogen addition to a half-hydrogenated intermediate is the rate-limiting step. Similar to electrogenerative hydrogenation on platinum (*4*) and to conventional catalytic hydrogenation of ethylene on palladium (*18*), the following elementary reaction steps can be considered:

$$C_2H_4 + 2^* \rightleftarrows \underset{*}{\overset{*}{CH_2—CH_2}}, \quad (I)$$

$$H^+ + e + * \rightleftarrows \underset{*}{H} \quad (II)$$

$$\underset{*}{\overset{*}{CH_2 - CH_2}} + e \rightleftarrows \underset{*}{CH_2—CH_3} + * \quad (III,III')$$

$$\underset{*}{\overset{*}{CH_2—CH_2}} + \underset{*}{H} \rightleftarrows \underset{*}{CH_2—CH_3} + 2^*, \quad (IV,IV')$$

$$CH_2=CH_2 + \underset{*}{H} \rightleftarrows \underset{*}{CH_2—CH_3}, \quad (V,V')$$

$$\underset{*}{CH_2—CH_3} + H^+ + e \rightarrow C_2H_6 + *, \quad (VI)$$

$$\underset{*}{CH_2—CH_3} + \underset{*}{H} \rightarrow C_2H_6 + 2^*, \quad (VII)$$

$$2\underset{*}{CH_2—CH_3} \rightarrow \underset{*}{\overset{*}{CH_2—CH_2}} + C_2H_6. \quad (VIII)$$

Since catalytic sites are in contact with electrolyte in electrocatalysis, adsorption (step (I)) or ethylene insertion (step (V)) should involve dissolved ethylene in the electrolyte. Reactant dissolution in a solvent and liquid-phase insertion are common steps in olefin homogeneous catalytic reactions (*19, 20*).

In order to eliminate some postulated steps, we calculated the reaction orders and transfer coefficients for possible combinations of the elementary steps, Table 3. In all sequences, the second hydrogen addition was considered to be rate limiting, as suggested by the reaction order in H^+ and by the Tafel slope for the electron-transfer process. The kinetic parameters of each model were calculated for either Langmuir or Temkin adsorption of reactants. Langmuir adsorption would be most applicable at total surface coverages $\theta_T \rightarrow 0$ or $\theta_T \rightarrow 1$. The latter would correspond to strong ethylene adsorption. Temkin adsorption conditions are considered for intermediate surface coverages $0.2 \leq \theta_T \leq 0.8$. Both adsorption isotherms are considered here because there is no information on the simultaneous electrosorption of eth-

TABLE 3

Estimated Kinetic Parameters for EGH of Ethylene over Palladium
Rate Equation: $i = nFk^0 P^a_{C_2H_4} C^b_{H^+} \exp(-\alpha EF/RT)$

Model	Steps	Langmuir adsorption							Temkin adsorption		
		$\theta_T \to 1$				$\theta_T \to 0$			$0.2 \le \theta_T \le 0.8$		
		a^a	a^b	b	α	a^c	b	α	a	b	α
A	I, III, VI	0	0.5	2	$1+\beta$	1	2	$1+\beta$	1	2	$1+\beta$
B	I, III, VIII	0	1	2	2	2	2	2	1	2	2
C	I, II, IV, VII	−1	0	2	2	1	2	2	0	2	2
D	I, II, IV, VIII	0	1	2	2	2	2	2	1	2	2
E	I, II, III, VII	−1	0	2	2	1	2	2	0	2	2
F	I, II, III, VIII	0	1	2	2	2	2	2	1	2	2
G	II, V, VII	NA				1	2	2	0	2	2

[a] One-site ethylene adsorption.
[b] Two-site ethylene adsorption.
[c] One- or two-site adsorption of ethylene.

ylene and hydrogen for a palladium–perchloric acid interface. Temkin adsorption of hydrogen was examined previously for ethylene electrogenerative hydrogenation on platinum (*4*).

Derivation of rate expressions for Langmuir adsorption of ethylene is straightforward. For example, model E, Table 3, yields for strong, two-site ethylene adsorption

$$i = nFk_{VII}{}^0 K_{II} K_{III} C_{H^+}{}^2 \exp(-2FE/RT). \quad (13)$$

Similarly, σ- or π-adsorption of ethylene with low surface coverage ($\theta_T \to 0$) gives for the same model

$$i = nFk_{VII}{}^0 K_I K_{II} K_{III} P_E C_{H^+}{}^2 \exp(-2FE/RT), \quad (14)$$

where P_E is the ethylene partial pressure and K_j represent adsorption equilibrium constants for steps (I)–(VIII). The rate dependence on ethylene partial pressure predicted by Eq. (14) is not, of course, in agreement with observed kinetics, Eq. (12).

For Temkin adsorption of hydrogen, reaction quasi-equilibrium for step (II) gives

$$K_{II} C_{H^+}(1 - \theta_T)\exp(-EF/RT) \exp[-f(\theta)/RT] = \theta_H, \quad (15)$$

where the surface interaction energy $f(\theta)$ is defined by

$$f(\theta) = \sum_J r_J \theta_J. \quad (16)$$

Here θ_J is the surface coverage of species J which has a free energy of adsorption r_J (*4*, *21*). While θ_J and θ_T can vary only between 0 and 1, the surface interaction energy can assume a significantly wide range of variation, depending on free energies of adsorption, r_J. The exponential terms in E and $f(\theta)$ of Eq. (15), then, will dominate the surface coverage characteristics for hydrogen adsorption compared to the linear terms θ_H and $(1 - \theta_T)$ (*4*, *21*). By considering these two linear terms relatively constant and by approximating them as unity (compared to the exponential terms) (*4*, *21*), Eq. (15) can be simplified to give

$$\exp[f(\theta)/RT] \simeq K_{II} C_{H^+} \exp(-EF/RT). \quad (17)$$

Equation (17) expresses the anticipated potential dependence of total surface coverage primarily through the variation of the hydrogen adsorption term in $f(\theta)$. This equation can be used now to derive kinetic

expressions, assuming that hydrogen Temkin adsorption determines the potential total surface coverage dependence of the electrocatalyst (*4*). For model E and nonactivated ethane adsorption (*4*) these assumptions yield

$$i = mFk_{VII}{}^{0}K_{II}{}^{2}C_{H}{}^{+2}\exp(-2FE/RT). \quad (18)$$

Temkin adsorption of hydrogen is considered predominant for the derivation of the kinetic parameters for models C, E, and G. In models A, B, D, and F the surface coverage by ethyl radicals is considered significant and following also a Temkin isotherm, in order to obtain partial agreement of the calculated parameters with the experimental ones. Equations similar to (15)–(17) can be written for ethyl radical adsorption as a function of potential and the surface interaction energy, to derive kinetic expressions. For the above derivations ethylene adsorption is assumed to be either a two-site σ-adsorption or a one-site π-adsorption (*4*).

Models in which the total surface coverage is negligible ($\theta_T \rightarrow 0$) apparently do not give agreement with the experimental results, especially with regard to the ethylene reaction order (see Eq. (14)). Models A, B, D, and F are consistent with the observed kinetics for strong, one-site adsorption, while C and E require the assumption of two-site ethylene adsorption. Models C, E, and G are also in agreement with experiment if Temkin adsorption of hydrogen is assumed.

In evaluating the reaction sequences above, some use was made of hydrogen adsorption data for palladium in contact with a sulfuric acid solution (*22, 23*). We have expressed reservation about H_2SO_4 (*4, 5*) but observations in this electrolyte can reveal some trends. In sulfuric acid the potential dependence of hydrogen surface coverage on palladium (*22*) is similar to that of platinum (*23*). Table 4 summarizes available adsorption data for both electrocatalysts. The surface coverage of hydrogen, θ_H, varies approximately linearly with potential between 0.25 and 0.10 V for palladium and 0.2 to 0.1 V for platinum. Surface heterogeneity or lateral interactions could give such linear $\theta_H - E$ dependence, Eq. (17) (*24*). For a Temkin isotherm, however, the heat of adsorption is expected to vary with coverage. This occurs on palladium for $\theta_H > 0.4$ and also on platinum, but there appears to be a relatively constant heat of absorption on palladium at lower coverage. Strongly adsorbed hydrogen atoms in this region (*22*) or hydrogen dissolution in the palladium lattice (*25*) may be reflected by this observation.

In general, hydrogen surface coverages for palladium and platinum are comparable in 0.5 and 2.3 *M* H_2SO_4, respectively. It is also noteworthy that the ethylene hydrogenation rate over palladium in 0.5 *N* $HClO_4$

TABLE 4

Hydrogen Adsorption on Platinum and Palladium Electrodes

Potential (V)	Platinum in 2.3 *M* H_2SO_4 (*23*)			Palladium in 0.5 *M* H_2SO_4 (*22*)		
	θ_H	ΔH_{ads} (kcal/mole)	ΔG°_{ads} (kcal/mole)	θ_H	ΔH_{ads} (kcal/mole)	ΔG°_{ads} 9kcal/mole)
0.3	0	−21.0	−4.5	0.03	−27.5	−3.8
0.25	0.08	−15.5		0.15	−27.5	
0.20	0.25	−12.6		0.31	−27.5	
0.15	0.44	−9.0		0.44	−27.2	
0.10	0.70	−6.5		0.60	−20.5	
0.075	0.82	−5.5		0.72	−16.2	

is approximately equal to the rate over platinum in 2 *N* $HClO_4$. It is, therefore, plausible to assume that adsorption of hydrogen atoms is important for ethylene hydrogenation over palladium and platinum in the low-potential region. If the free energy and enthalpy of adsorption of ethylene remain relatively constant with potential on palladium, as they do on platinum (*4*), hydrogen adsorption will impose its potential–surface coverage behavior on the ethylene reaction. Similarly, the hydrogen adsorption isotherm will govern the reaction if insertion of dissolved, nonadsorbed ethylene takes place, Eq. (V).

Reduction of ethylene in a deuterium-labeled electrolyte might reveal possible preference for some of the sequences of the hydrogenation steps of Table 3. Our previous isotopic exchange results with platinum suggest some mechanism similarities between reduction at positive potentials and gas-phase catalytic hydrogenation (*4, 5*). Therefore, information on catalytic deuteration of ethylene on palladium could suggest possible elementary steps in the electrogenerative cell.

Bond *et al.* (*18*) observed substantial olefin exchange but no HD formation upon reacting ethylene and deuterium gases on a conventional Pd-on-alumina catalyst. The probability of occurrence of each postulated step indicated that addition of a second hydrogen to an adsorbed ethyl radical was slow, in accord with the present electrocatalytic kinetic results. Based on the selectivity for hydrogen or deuterium addition to ethyl radicals, Bond *et al.* suggested that ethane formation on palladium proceeds primarily through surface exchange between adsorbed ethylene and ethyl radicals and eventual ethyl radical disproportionation, step (VIII) (*18*). Step (VIII) was also found rate limiting on platinum electrocatalysts at high potentials and low rates, with step (VII) becoming important at low potentials and high rates (*4, 5*). Increasing significance of surface reaction (VII) is expected with decreasing potential, as adsorbed hydrogen becomes readily available on the surface or in the palladium lattice (see coverage data, Table 4).

The major path for the first hydrogen addition does not seem to be the same for palladium and platinum. On the latter, a "concerted" hydrogen ion addition with simultaneous electron transfer (step (III)) appears to be the first step (*4, 5*). If this occurred also on palladium, selectivity differences would not be anticipated upon reduction of halogen-substituted alkenes on these metals. The observed differences in selectivity for reduction of haloalkenes can be explained by a "surface insertion mechanism" for palladium to reduce the double bond, Eq. (19), and a "concerted mechanism" for platinum, Eq. (20), where only cleavage occurs (*2*):

$$[CH_2{=}CHF] + [H] \rightleftarrows [CH_2CH_2F] \xrightarrow{+[H]} CH_3CH_2F, \quad (19)$$

$$[CH_2{=}CHF] \xrightarrow[-e]{-H^+} [CH_2{=}\overset{\delta^+}{C}H_2\text{-----}\overset{\delta^-}{F}] \xrightarrow[-e]{+H^+} [CH_2{=}CH_2] + HF. \quad (20)$$

Similar steps can also be anticipated for unsubstituted alkenes. Palladium participation in insertion reactions is well known in homogeneous catalysis (*19, 20*). Ethylene insertion may be facilitated on palladium by the presence of hydrogen strongly adsorbed on the surface or dissolved in the lattice (*25*).

From selectivity and deuterium exchange considerations, then, together with other arguments presented here, it appears that the predominant initiating reactions on palladium electrocatalyst are: insertion of dissolved ethylene to surface adsorbed hydrogen (step (V)) or ethylene adsorption followed by surface reaction with hydrogen atoms (steps (I), (IV)). Since some cleavage of haloalkenes is also observed on palladium (10–40% depending on potential (*2*)), reaction (III) can also contribute to the overall ethylene hydrogenation reaction by

an equivalent amount. Reactions (III) and (V) may take place on different catalytic sites since the former initially involves only adsorbed ethylene and the latter only adsorbed hydrogen. With the relative coverage of each site type varying with potential, the contribution of each path to the overall reaction would be potential dependent. Step (III), then, should be most important at potentials above ~0.2 V where cleavage of halides is significant (*2*) and where hydrogen adsorption is limited.

The nature of the rate-limiting, second hydrogen addition is probably potential dependent too. At potentials higher than ~0.25 V the availability of hydrogen atoms on the surface or in the lattice is low (*4*). Thus ethyl radical disproportionation on palladium (step (VIII)) should be important as with platinum in the same potential region (*4*). At lower potentials (<0.18 V), discharge of H^+ and Temkin hydrogen adsorption can make the contribution of reaction (VII) important.

The proposed ethylene electrogenerative hydrogenation scheme and the previously discussed adsorption isotherms are consistent with our experimental kinetic parameters. This scheme also can explain observed differences in reaction rate and selectivity of double bond reduction on palladium and platinum electrocatalysts.

Because of the faster reaction rate on palladium at a given potential, the energy generated by ethylene reduction on this electrode is about an order of magnitude higher than on platinum. To achieve comparable energy outputs, either the platinum catalytic load should be increased by 115% or a fourfold increase in acid electrolyte concentration is necessary, as suggested by previous kinetic and electrocatalytic results (*4*). However, the catalytic advantage of palladium is offset somewhat by inefficient catalyst utilization at low substrate partial pressures.

CONCLUSIONS

Palladium-black porous electrocatalysts promote the ethylene hydrogenation reaction at a faster rate than on platinum at equivalent potentials. The reaction is zero order in ethylene and second order in hydrogen ions for both catalysts. However, pore diffusion becomes relatively slow on our palladium electrocatalyst at low ethylene partial pressures. This simple reaction demonstrates the feasibility of successful kinetic analysis with porous electrocatalysts using a single pore model. The proposed model predicts the change in Tafel slope and location of potential–current density curves with slow pore diffusion superimposed on power-law electrode kinetics.

The ethylene reaction on palladium probably proceeds by olefin insertion to adsorbed hydrogen atoms or surface reaction between adsorbed ethylene and hydrogen. In parallel to this, a potential-dependent, electrochemical "concerted" proton addition may take place, possibly on different catalytic sites. These reactions are followed by a rate-limiting hydrogen transfer to ethyl radicals at the surface or by ethyl disproportionation depending on potential. The lower overpotential on palladium than on platinum may be a result of mechanism difference and of the tendency for palladium to adsorb or dissolve hydrogen at more positive potentials than platinum.

APPENDIX: NOMENCLATURE

A_g	Exposed geometric area of the electrocatalyst (cm^2)
C_J	Concentration of species J ($mole/cm^3$)
$\mathscr{D}_J$	Diffusion coefficient of J (cm^2/s)
E	Electrode potential vs NHE (V)
E_C	Corrected cathode voltage (V)
F	Faraday's constant ($A \cdot s/eq$)
$f(\theta)$	Surface interaction energy, Eq. (16), (kcal/mole)
h	Electrochemical Thiele modulus
i	Current density (A/cm^2)
j	Intrinsic order of species J
j'	Apparent order of species J
K	Equilibrium constant of indicated reaction step

k_J^0	Surface rate constant at zero potential (mole^{i-j} cm^{3j-2} s^{-1})
L	Pore length (cm)
n	Number of electrons
$P_{C_2H_4}$	Partial pressure of ethylene (atm)
R	Gas constant (J/mole · °K)
R_i	Cell internal resistance (ohm)
R_p	Pore radius (cm)
r_J	Free energy of adsorption of species J (kcal/mole)
T	Temperature (°K)
X^*	Dimensionless axial coordinate ($=X/L$)

Greek Letters

α	Intrinsic transfer coefficient
ϵ	Electrochemical effectiveness factor
θ_J	Catalyst surface coverage
Ψ_J	Dimensionless concentration of J ($=C_j/C_{j\infty}$)

Subscripts

g	Geometric area value
J	Species J
L	Limiting value
∞	Bulk or intrinsic value

ACKNOWLEDGMENTS

We thank the National Science Foundation and the University of Wisconsin for support of this work.

REFERENCES

1. Langer, S. H., and Landi, H. P., *J. Amer. Chem. Soc.* **85,** 3043 (1963); **86,** 4694 (1964).
2. Sakellaropoulos, G. P., and Langer, S. H., *J. Catal.* **44,** 25 (1976).
3. Liebhafsky, H. A., and Cairns, E. J., "Fuel Cells and Fuel Batteries." Wiley, New York, 1968.
4. Langer, S. H., and Sakellaropoulos, G. P., *J. Electrochem. Soc.* **122,** 1619 (1975).
5. Langer, S. H., Feiz, I., and Quinn, C. P., *J. Amer. Chem. Soc.* **93,** 1092 (1971).
6. Sakellaropoulos, G. P., and Langer, S. H., *AIChE J.* **24,** 1115 (1978).
7. Sokol'skii, D. V., and Druz, W. A., *Dokl. Akad. Nauk SSSR* **73,** 949 (1950).
8. Beck, F., *Ber. Bunsenges. Phys. Chem.* **69,** 199 (1965).
9. Beck, F., and Gerischer, H., *Z. Elektrochem* **65,** 504 (1961).
10. Burke, L. D., Kemball, C., and Lewis, F. A., *Trans. Faraday Soc.* **60,** 913 (1964); **60,** 919 (1964).
11. Haldeman, R. G., Colman, W. P., Langer, S. H., and Barber, W. A., *Advan. Chem. Ser.* **47,** 116 (1965).
12. Vetter, K. J., "Electrochemical Kinetics: Theoretical and Experimental Aspects," pp. 119, 143. Academic Press, New York, 1967.
13. Aris, A., "Elementary Chemical Reactor Analysis," pp. 137, 138. Prentice-Hall, Englewood Cliffs, N.J., 1969.
14. Petersen, E. E., "Chemical Reaction Analysis," pp. 51–57. Prentice-Hall, Englewood Cliffs, N.J., 1965.
15. Will, F. G., *J. Electrochem. Soc.* **110,** 152 (1963).
16. Fujikawa, K., Kita, H., and Miyahara, K., *J. Chem. Soc. Faraday Trans. I* **69,** 481 (1973).
17. Sakellaropoulos, G. P., and Langer, S. H., *J. Electrochem. Soc.* **124,** 1548 (1977).
18. Bond, G. C., Phillipson, J. J., Wells, P. B., and Winterbottom, J. M., *Trans. Faraday Soc.* **62,** 443 (1966).
19. Basolo, F., and Pearson, R. G. "Mechanism of Inorganic Reactions," 2nd ed., pp. 596–598. Wiley, New York, 1967.
20. Halpern, J., *Chem. Eng. News* **44,** 68 (Oct. 31, 1966).
21. Conway, B. E., and Gileadi, E., *Trans. Faraday Soc.* **58,** 2493 (1962).
22. Vert, Zh. L., Mosevich, I. A., and Tverdovsky, I., *Dokl. Akad. Nauk SSSR* **140,** 149 (1961).
23. Böld, M., and Breiter, M., *Z. Elektrochem.* **64,** 897 (1960).
24. Breiter, M., "Electrochemical Processes in Fuel Cells," pp. 52–56. Springer-Verlag, Berlin/Heidelberg, 1969.
25. Hull, M. N., and Lewis, F. A., *Trans. Faraday Soc.* **64,** 2472 (1968).